Chiang Mai J. Sci. 2018; 45(5) : 2005-2014
http://epg.science.cmu.ac.th/ejournal/
Contributed Paper

Effect of Concentration of Citric Acid on Size and Optical Properties of Fluorescence Graphene Quantum Dots Prepared by Tuning Carbonization Degree

Pichitchai Pimpang* [a], Rattiphorn Sumang [a] and Supab Choopun [b]
[a] Faculty of Science and Technology, Pibulsongkram Rajabhat University, Phitsanulok 65000, Thailand.
[b] Department of Physics and Materials Science, Faculty of Science, Chiang Mai University, Chiang Mai 50200, and ThEP center, CHE, Bangkok 10400, Thailand.
* Author for correspondence; e-mail: p.pimpang@gmail.com

Received: 1 November 2017
Accepted: 30 April 2018

ABSTRACT

In this work, the effect of concentration of citric acid precursor on size and optical properties of graphene quantum dots has been investigated. Citric acid precursor (CA) was obtained at different concentrations of 0.1, 0.2, 0.5, and 1.0 M by dissolving citric acid monohydrate powder in ethanol. The CA was then carbonized to form graphene quantum dots (GQDs) at a temperature of 250 °C. Based on observation by naked eye, the color of CA changed from an initial colorless solution to melted yellow and it exhibited strong blue fluorescence under excitation wavelength of 365 nm. These results implied formation of GQDs. Characterizations of GQDs were performed by using dynamic light scattering, FT-IR spectroscopy, UV-vis spectroscopy, and fluorescence spectroscopy. The typical morphology of GQDs was carried out by utilizing transmission electron microscopy. It was found that average size of GQDs decreased on elevating the CA concentration. The absorbance spectra exhibited strong excitonic absorption bands in ultraviolet region and their absorption edge decreased from 327 to 314 nm on increasing the CA concentration. The fluorescence spectra exhibited bright fluorescence bands in visible region and their peak fluorescence decreased from 459 nm to 443 nm with increasing CA concentration. Optical properties of GQDs confirmed their non-zero band gap and tunable fluorescence property *via* synthesis condition. Accordingly, size-dependent optical properties of fluorescence GQDs could be explained in term of quantum size effect. These results potentially have novel applications in bioimaging, biosensing, and light emitting diodes.

Keywords: graphene, quantum size effect, fluorescence, optical properties

1. INTRODUCTION

Graphene quantum dots (GQDs) have caught attention due to their exceptional electronic, surface chemistry, and tunable fluorescence properties, which benefit from its unique zero-dimensional (0D) nanometer-sized particle of graphene, edge-shape effect, and quantum confinement effect [1, 2]. It is well-known that GQDs have a graphene structure inside the dots, which still possesses several unique properties that similar to graphene such as high specific surface area (~2630m^2/g) [3-6], excellent electrical conductivity (~1738 siemens/m) [7, 8], strong mechanical strength (~1100 GPa) [8, 9], and unique thermal conductivity (~5000 W/m/K)[10, 11]. Notably, graphene film does not has optical emission due to its zero band gap, which limits its applications [12]. The GQDs show characteristic properties such as size-dependent properties of quantum dots [13, 14], tunable fluorescence in the visible spectra range [15, 16], and biocompatibility [16] due to their single or few layers of sp^2 hybridized carbon atoms arranged in a honeycomb lattice, non-zero band gap and nanometer-sized particles. Therefore, it has great potential applications in biosensing and bioimaging for its low toxicity in vivo [3, 17-19], photovoltaics [14, 20, 21], light-emitting diodes [22], and sensors [3, 13, 23]. In addition, as reported, most applications have been focused on the optical properties of GQDs [21]. GQDs are expected to show tunable photoluminescence (PL) colors on changing band gap *via* surface modifications and different synthesis conditions [21]. Thus the controllable synthesis of GQDs is devoted to the development of their applications using various approaches [21].

There are many approaches to prepare GQDs, which can be generally classified into two categories: top-down and bottom-up approaches. The top-down approach involves cutting down bulk carbonaceous materials (i.e., graphene sheets [24] and carbon nanotubes [25] and bulkgraphite [26]) into nanometer-sized particle and involves harsh reaction conditions. Graphene oxide is also a good candidate because the oxygen-containing functional groups on graphene surface can easily be broken down into nanometer-sized and single-layered particle of GQDs [24]. However, The top-down approach has limitations due to requirement of multistep and post-treatment with surface passivating agents [27], and don't generally allow precise morphology and size distribution of the products. The bottom-up approach is appropriate for controlling the size of GQDs as it involves building blocksfrom atomormolecule precursors, and it uniformly controls the size which directly relates to the band gap of quantum dots [21]. There are reports about GQDs synthesis *via* the bottom-up approach such aspyrolysis and carbonization [28, 29], hydrothermal process [30], exfoliation process [31, 32], molecules self-assembly [31], microwave-assisted reduction [33] and electrochemical method [34]. Among them, carbonizationhas obvious advantages in adjusting the composition andphysical properties of GQDs [29]. Basically, carbonization is method that involves conversion of organic precursors into carbon through pyrolysis distillation. The precursors can be selected from diversified organic molecules such as citric acid, glucose, sucrose, glycol, ascorbic acid, etc. Dong et al. synthesized GQDs *via* the facile carbonization of citric acid [28]. In a typical GQDs synthesis, 2 g of colorless citric acid powderis heated at 200 °C under normal atmospheric condition. About 5 min later, the citric acid powder is

changed to orange melted liquid. It is found that the synthesized GQDs have thickness about 0.5-2.0 nm. Interestingly, synthesized GQDs exhibit blue fluorescence, which correlate to their non-zero band gap. In addition, the rapid GQDs synthesis through tuning the carbonization of citric acid powder has been reported by Naik et al. [29], who studied the effect of different pH on the formation of GQDs. To study the effect of pH on the formation of GQDs, 5 g of solid citric acid powder is heated and melted until it changed to dark melted orange. NaOH solution is then added in the melted orangeat different pH ranging from 8 to 12 under room temperature condition. It is found that the pH of 9 exhibits optimum condition for the formation of GQDs due toits minimum size of about 1.5 nm. The effect of concentration of citric acid precursoron size and optical properties of GQDs has still not been reported.

This work, the effect of concentration of citric acid on size and optical properties of graphene quantum dots has been investigated. Graphene quantum dots (GQDs) were prepared by tuningthe carbonization degree of citric acid at 250 °C. A tuningthe carbonization degree of small organic precursor has obvious advantages in uniformly controlling the size, which directly relates to the band gap of quantum dots. However, an optimized temperature for carbonization of citric acid precursor (CA) is still no report. As described at elsewhere report[28], an incompletely carbonized CA is obtained at temperature of 200 °C. Hence, the carbonized temperature of 250 °C was expected for developing effective method to prepare GQDs. CA was prepared at different concentration of 0.1, 0.2, 0.5, and 1.0 M by dissolving citric acid monohydrate powder in ethanol. Ethanol is promising candidate for solubility of citric acid [35]. Microstructures of GQDs were obtained by dynamic light scattering (DLS), transmission electron microscopy (TEM) and fourier transform infrared (FT-IR) spectroscopy. Optical properties of GQDs were analyzed by UV-vis spectroscopy, and fluorescence spectroscopy.

2. MATERIALS AND METHODS

To investigate the effect of concentration of citric acid precursor on the formation of graphene quantum dots, graphene quantum dots (GQDs) were prepared by tuning the carbonization degree of citric acid precursor at different concentrations. Firstly, citric acid precursor (CA) was prepared at different concentrations of 0.1, 0.2, 0.5, and 1.0 M by dissolving citric acid (monohydrate) powder in an ethanol. In a typical precursor of preparation, 0.1 M CA was prepared by adding 2.1120 g of citric acid monohydrate powder (99.5%, Loba Chemie; MW 210.14 g/mol) in the presence of 100 mL of an ethanol (99.5%, Merck). The mixture was stirred at room temperature until colorless solution was obtained. Then, a 500 mL pyrex beaker was heated at a constant temperature of 250 °C using a hot plate stirrer (IKA C-MAG HS7). After that, 100 mL of CA solution was added dropwise into a heated beaker to maintain the temperature. According to heating CA solution, an ethanol was evaporated and the color of CA precursor changed from an initial colorless solution to melted yellow. The resulting melted yellow that observed by naked eyesand strong blue fluorescence under excitation wavelength at 365 nm implied the formation of GQDs. Finally, the synthesized GQDs were stored at to room temperature before an ethanol was added to maintain initial volume of 100 mL.

The microstructures of GQDs were

obtained by dynamic light scattering (DLS, Malvern ZetasizerNano S), transmission electron microscopy (TEM, Philips FEI Tecnai 12) and fourier transform infrared (FT-IR) spectroscopy (Thermo scientific Nicolet™iS). Optical properties of GQDs were analyzed by UV-vis spectroscopy (Shimadzu UV-2450), and fluorescence spectroscopy (ShimadzuRF-6000). DLS size distribution was measurement in the range of 0.3 nm - 10 µm. A typical sample for TEM was prepared by drying naturally a drop of solution containing GQDs at room temperature on a carbon-coated copper grid. FT-IR spectra were observed in the range of 500-4000 cm^{-1}. UV-vis absorption spectra of GQDs were recorded in the range of 200-700 nm. Excitation-emission contour maps of GQDs were performed by utilizing excitation wavelength in the range of 300-400 nm. Fluorescence spectra were assessed in the range of 400-700 nm at excitation wavelength of 365 nm.

3. RESULTS AND DISCUSSION

Typical FT-IR spectra of citric acid precursor (CA) and graphene quantum dots (GQDs) prepared using 1.0 M of CA were shown in Figure 1. The GQDs prepared using 1.0 M of CA was demonstrated to represent to the microstructure for obtained GQDs that prepared using 0.1, 0.2, 0.5, and 1.0 M of CA because all vibrational modes was quite similar. It was found that CA showed the broadening of O-H stretching (R-C(O)-OH) at around 3290.12 cm^{-1}, C=O stretching (C(O)-OH) at1721.69 cm^{-1}, C-OH stretching at 1105.85 cm^{-1}, and CH_2 rocking at 778.78 cm^{-1}. The result is attributed to the vibrational modes of citric acid molecule [28]. Contrarily, FT-IR spectra of GQDs has no detectable O-H stretching, implying a decomposition of citric acid (monohydrate) molecule ($(COOH)CH_2COOH \times H_2O$) and complete carbonization can be achieved. Additionally, the GQDs exhibited the C-H stretching at 2983.34 cm^{-1}, C=O stretching (C(O)-OH) at 1725.18 cm^{-1} [29], C-OH stretching at and 1182.28 cm^{-1}, and C-O stretching at and 1022.34 cm^{-1} [28], implying the vibration of hydroxyl group and carboxyl group that functionalized onto crystalline GQDs. It can be seen that FT-IR spectra of GQDs has no detectable C-O-C group (stretching vibration), suggesting no characteristic feature for graphene oxide that C-O-C groups are abundant on the graphene basal planes. Accordingly, the microstructure investigation of GQDs was carried out using transmission electron microscopy (TEM).

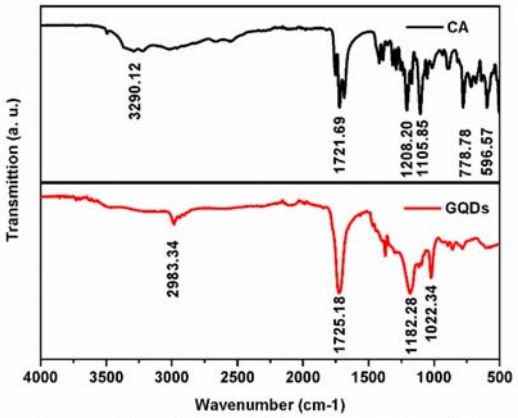

Figure 1. Typical FT-IR spectra of citric acid (CA) and graphene quantum dots (GQDs) prepared using 1.0 M of CA.

Typical TEM image of GQDs has been shown in Figure 2. The GQDs prepared using 1.0 M of CA shows morphology for GQDs prepared using 0.1, 0.2, 0.5, and 1.0 M of CA and the morphology appeared quite similar. It was found that GQDs exhibited monodispersed distribution with an average lateral size of 1.50±0.48 nm. High-resolution TEM images demonstrated the morphology of the nano-sheet to have

an interlayer spacing of about 0.4 nm, which was larger than that of bulk graphite (0.335 nm) [36]. A larger interlayer spacing may be due to the presence of the functional groups that enlarge the basal plane spacing of the GQDs [12].

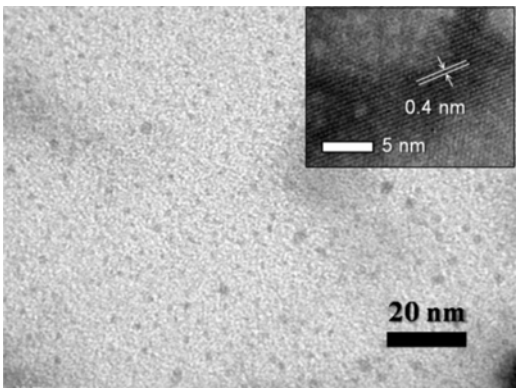

Figure 2. Typical TEM image of GQDs prepared using 1.0 M of CA. Inset: high-magnification TEM images demonstrated the morphology of the nano-sheet with an interlayer spacing of about 0.4 nm.

Figure 3 shows DLS size distributions of GQDs prepared using CA at different concentrations of 0.1, 0.2, 0.5, and 1.0 M. In all cases, size distribution was assessed using ten repeated measurements, which majority of that size had detectable. It was clear that the average size of GQDs decreased from 0.78 to 0.68 nm on elevating the CA concentration. In addition, size distribution tended to decrease on increasing the CA concentration. This was in good agreement with a previous report [37] which showed that a higher initial concentration of precursor results in smaller nanometer-sized particles. It should be noted that the average size was measured to be less than 1 nm, which is due the average in all dimensions (horizontal and vertical) of GQDs plates. Therefore, the effect of concentration of citric acid precursor on size of GQDs could be explained in term of nucleation and growth.

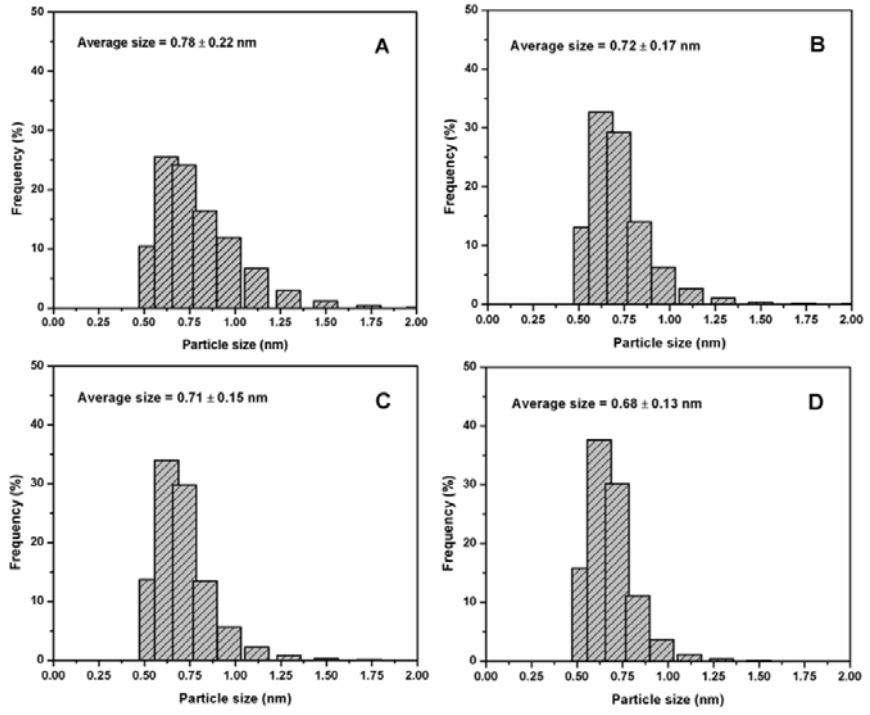

Figure 3. DLS size distributions of GQDs prepared using different concentrations of citric acid: 0.1 M (A), 0.2 M (B), 0.5 M (C), and 1.0 M (D).

Optical absorption of CA and GQDs were assessed using UV-vis spectra (Figure4). GQDs exhibited strong excitonic absorption bands in ultraviolet region and their absorption edge decreased from 327 to 314 nm with increasing CA concentration. Furthermore, GQDs showed absorption bands in visible region and their absorption edge decreased from 390 to 380 nm with increasing CA concentration. The ultraviolet absorption (~320 nm) is related to the electron transitions from n to π^* of C=C and the visible absorption related to the partial conjugated π electrons in the layered GQDs [12, 38]. Thus, blue-shift in optical absorption was due to their decreasing average size and it was in agreement with other report [21].

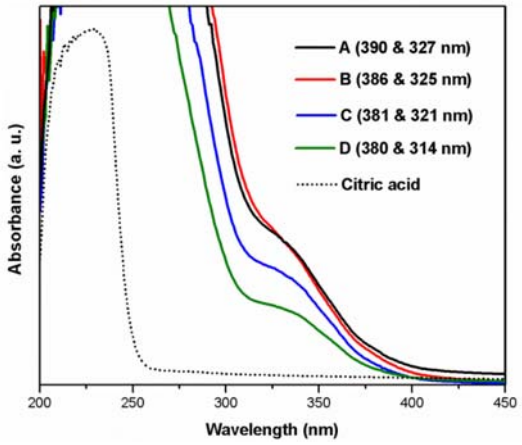

Figure 4. UV-vis absorbance spectra of GQDs prepared using different concentrations of citric acid: 0.1 M (A), 0.2 M (B), 0.5 M (C), 1.0 M (D) and 0.1 M citric acid (dot line).

Optical emission properties of GQDs were measured using fluorescence spectroscopy. Figure 5 shows excitation-emission contour maps of GQDs prepared using CA at different concentrations of 0.1, 0.2, 0.5, and 1.0 M. Bright area corresponds to high emission intensity. It was found that maximum excitation wavelength decreased from about 372 to 342 nm by increased CA concentration. Interestingly, maximum emission wavelength decreased from about 434 to 431 nm by increased CA concentration. Therefore, Fluorescence spectra of GQDs were observed in visible region. Fluorescence spectra of obtained GQDs are shown in Figure 6. A thorough understanding the emission spectra of GQDs, fluorescence characterization indicated that the GQDs can emit strong blue fluorescence under excitation wavelength at 365 nm [18, 23, 28, 39]. It was found that the peak fluorescence decreased from 459 nm to 443 nm with increasing CA concentration. Hence blue-shift of optical emission was observed due to their decreasing average size and it was good in agreement with other reports [21, 40]. Accordingly, optical properties of GQDs confirmed their non-zero band gap and tunable fluorescence property *via* synthesis condition. Size-dependent optical properties of fluorescence GQDs could be explained in term of quantum size effect.

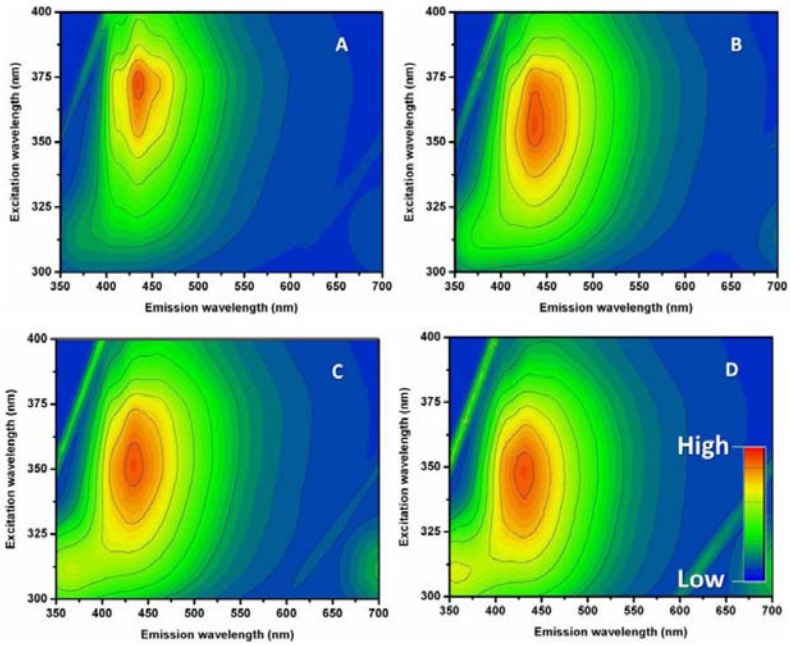

Figure 5. Excitation-emission contour maps of GQDs prepared using different concentrations of citric acid: 0.1 M (A), 0.2 M (B), 0.5 M (C), 1.0 M (D). Bright area corresponds to high emission intensity.

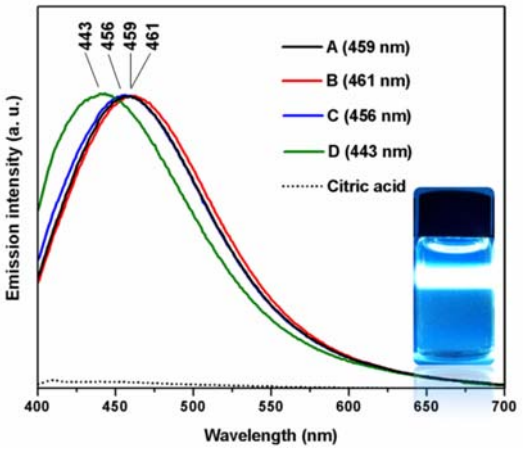

Figure 6. Fluorescence spectra of GQDs prepared using different concentrations of citric acid: 0.1 M (A), 0.2 M (B), 0.5 M (C) and 1.0 M (D). Fluorescence spectra were observed under excitation wavelength of 365 nm.

The mechanism of GQD growth was proposed as in the following steps. First, C-OH, C(O)-OH and CH_2 of citric acid molecules $(COOH)CH_2COOH{\cdot}H_2O$) were decomposed to form carbon precursor *via* the facile carbonization of citric acid. Next, nucleation of carbon nuclei (seeds) can be explained by introducing nucleation and growth of nanoparticles in solution [41]. The process of homogeneous nuclei formation can be considered by taking the total free energy of a nanoparticle (ΔG) defined as the sum of the surface free energy and the bulk free energy (ΔG_V) as:

$$\Delta G = \frac{4}{3}\pi r^3 \Delta G_V + 4\pi r^2 \gamma \quad (1)$$

$$\Delta G_V = -\frac{k_B T \ln(S)}{\Omega} \quad (2)$$

Where γ is the surface free energy, Ω is molar volume, T is temperature, and k_B is the Boltzmann constant and the supersaturation of the solution (S). The critical radius (r_{crit}), and the maximum energy barrier (ΔG_{crit}) can be simply obtained at $d\Delta G/dr = 0$ as:

$$\Delta G_{crit} = \frac{4}{3}\pi\gamma r_{crit}^2 \quad (3)$$

$$r_{crit} = \frac{2\gamma\Omega}{k_B T \ln(S)} \quad (4)$$

From Eq. (4), critical radius corresponds to the minimum size of particle, which is formed in solution without redissolved. Thus, three experimental parameters can be varied: the surface free energy (γ), temperature (T), and supersaturation (S). Finally, nano-sized graphene was growth with a minimum surface free energy. In this work, GQDs synthesis with carbonization of CA at constant temperature of 250 °C can be achieved. An average size and size distribution of GQDs were decreased with increasing an initial CA concentration, which was attributed supersaturation parameter; S. Therefore, the formation of GQDs could be explained in term of nucleation and growth.

4. CONCLUSIONS

Graphene quantum dots (GQDs) have been prepared by tuningthe carbonization degree of citric acidprecursor (CA) at different concentrations of 0.1, 0.2, 0.5 and 1.0 M. Naked eye observation indicate a strong blue fluorescence under excitation wavelength of 365 nm, and implied the formation of GQDs. It was found that average size of graphene decreased on elevating the CA concentration. Therefore, the effect of CA concentration on size of GQDs could be explained in term of nucleation and growth. Blue-shift of optical absorption and optical emission were likley due to their decreasing average size. Additionally, peak fluorescence decreased by increased CA concentration. The optical properties of GQDs confirmed their non-zero band gap and tunable fluorescence property *via* synthesis condition. Accordingly, size-dependent optical properties of fluorescence GQDs could be explained in term of quantum size effect.

ACKNOWLEDGMENTS

Authors would like to kindly acknowledge the Science Center Faculty of Science and Technology, Pibulsongkram Rajabhat University for advanced analytical equipment. Thanks are given to Dr. Nitish Kumarfor his help in editing the manuscript.

REFERENCES

[1] Zhang R., Qi S., Jia J., Torre B., Zeng H., Wu H. and Xu X., *J. Alloy. Compd.*, 2015; **623**: 186-191. DOI 10.1016/j.jallcom.2014.10.105.

[2] Zhu S., Song Y., Wang J., Wan H., Zhang Y., Ning Y. and Yang B., *Nano Today*, 2017; **13**: 10-14. DOI 10.1016/j.nantod.2016.12.006.

[3] Sun H., Wu L., Wei W. and Qu X., *Mater. Today*, 2013; **16(11)**: 433-442. DOI 10.1016/j.mattod.2013.10.020.

[4] Stoller M.D., Park S., Zhu Y., An J. and Ruoff R.S., *Nano Lett.*, 2008; **8(10)**: 3498-3502. DOI 10.1021/nl802558y.

[5] Ang P.K., Chen W., Wee A.T.S. and Loh K.P., *J. Am. Chem. Soc.*, 2008; **130(44)**: 14392-14393. DOI 10.1021/ja805090z.

[6] Wang Y., Shi Z., Huang Y., Ma Y., Wang C., Chen M. and Chen Y., *J. Phys. Chem. C*, 2009; **113(30)**: 13103-13107. DOI 10.1021/jp902214f.

[7] Hasanzadeh M., Karimzadeh A., Sadeghi S., Mokhtarzadeh A., Shadjou N. and Jouyban A., *J. Mater. Sci.-Mater. El.*, 2016; **27(6)**: 6488-6495. DOI 10.1007/s10854-016-4590-6.

[8] Yang Y., Asiri A.M., Tang Z., Du D. and Lin Y., *Mater. Today*, 2013; **16(10)**: 365-373. DOI 10.1016/j.mattod.2013.09.004.

[9] Lee C., Wei X., Kysar J.W. and Hone J., *Science*, 2008; **321(5887)**: 385-388. DOI 10.1126/science.1157996.

[10] An X., Butler T.W., Washington M., Nayak S.K. and Kar S., *ACS Nano*, 2011; **5(2)**: 1003-1011. DOI 10.1021/nn102415c.

[11] Balandin A.A., Ghosh S., Bao W., Calizo I., Teweldebrhan D., Miao F. and Lau C.N., *Nano Lett.*, 2008; **8(3)**: 902-907. DOI 10.1021/nl0731872.

[12] Tang L., Ji R., Li X., Bai G., Liu C.P., Hao J., Lin J., Jiang H., Teng K.S., Yang Z. and Lau S.P., *ACS Nano*, 2014; **8(6)**: 6312-6320. DOI 10.1021/nn501796r.

[13] Shen J., Zhu Y., Yang X. and Li C., *Chem. Commun.*, 2012; **48(31)**: 3686-3699. DOI 10.1039/C2CC00110A.

[14] Zhang Z., Zhang J., Chen N. and Qu L., *Energy Environ. Sci.*, 2012; **5(10)**: 8869-8890. DOI 10.1039/C2EE22982J.

[15] Sapkota B., Benabbas A., Lin H.Y.G., Liang W., Champion P. and Wanunu M., *ACS Appl. Mater. Int.*, 2017; **9(11)**: 9378-9387. DOI 10.1021/acsami.6b16364.

[16] Alam Sk.M., Ananthanarayanan A., Huang L., Lim K.H. and Chen P., *J. Mater. Chem. C*, 2014; **2(34)**: 6954-6960. DOI 10.1039/C4TC01191K.

[17] Zhu S., Zhang J., Qiao C., Tang S., Li Y., Yuan W., Li B., Tian L., Liu F., Hu R., Gao H., Wei H., Zhang H., Sun H. and Yang B., *Chem. Commun.*, 2011; **47(24)**: 6858-6860. DOI 10.1039/C1CC11122A.

[18] Wang L., Li W., Wu B., Li Z., Wang S., Liu Y., Pan D. and Wu M., *Chem. Eng. J.*, 2016; **300**: 75-82. DOI 10.1016/j.cej.2016.04.123.

[19] Zhang J., Ma Y.Q., Li N., Zhu J.L., Zhang T., Zhang W. and Liu B., *J. Nanomater.*, 2016; **2016**: 1-9. DOI 10.1155/2016/9245865.

[20] Li X., Chen W., Zhang S., Wu Z., Wang P., Xu Z., Chen H., Yin W., Zhong H. and Lin S., *Nano Energy*, 2015; **16**: 310-319. DOI 10.1016/j.nanoen.2015.07.003.

[21] Bak S., Kim D. and Lee H., *Curr. Appl. Phys.*, 2016; **16(9)**: 1192-1201. DOI 10.1016/j.cap.2016.03.026.

[22] Son D.I., Kwon B.W., Park D.H., Seo W.S., Yi Y., Angadi B., Lee C.L. and Choi W.K., *Nat. Nanotechnol.*, 2012; **7(7)**: 465-471. DOI 10.1038/nnano.2012.71.

[23] Liu J.J., Chen Z.T., Tang D.S., Wang Y.B., Kang L.T. and Yao J.N., *Sens. Actuators B-Chem.*, 2015; **212**: 214-219. DOI 10.1016/j.snb.2015.02.019.

[24] Pan D., Zhang J., Li Z. and Wu M., *Adv. Mater.*, 2010; **22(6)**: 734-738. DOI 10.1002/adma.200902825.

[25] Li F., Kou L., Chen W., Wu C. and Guo T., *NPG Asia Mater.*, 2013; **5**: e60. DOI 10.1038/am.2013.38.

[26] Kwon W., Kim Y.H., Lee C.L., Lee M., Choi H.C., Lee T.W. and Rhee S.W., *Nano Lett.*, 2014; **14(3)**: 1306-1311. DOI 10.1021/nl404281h.

[27] Gao W., The Chemistry of Graphene Oxide in Graphene Oxide: Reduction Recipes, Spectroscopy, and Applications, Springer, 2015: 61-95. DOI 10.1007/978-3-319-15500-5_3.

[28] Dong Y., Shao J., Chen C., Li H., Wang R., Chi Y., Lin X. and Chen G., *Carbon*, 2012; **50(12)**: 4738-4743. DOI 10.1016/j.carbon.2012.06.002.

[29] Naik J.P., Sutradhar P. and Saha M., *J. Nanostruct. Chem.*, 2017; **7(1)**: 85-89. DOI 10.1007/s40097-017-0222-9.

[30] Tang L., Ji R., Cao X., Lin J., Jiang H., Li X., Teng K.S., Luk C.M., Zeng S., Hao J. and Lau S.P., *ACS Nano*, 2012; **6(6)**: 5102-5110. DOI 10.1021/nn300760g.

[31] Qu D., Zheng M., Zhang L., Zhao H., Xie Z., Jing X., Haddad R.E., Fan H. and Sun Z., *Sci. Rep.-UK*, 2014; **4**: 5294. DOI 10.1038/srep05294.

[32] Kang S.H., Mhin S., Han H., Kim K.M., Jones J.L., Ryu J.H., Kang J.S., Kim S.H. and Shim K.B., *Sci. Rep.-UK*, 2016; **6**: 38423. DOI 10.1038/srep38423.

[33] Oliver Kappe C., *Angew. Chem. Int. Ed.*, 2004; **43**: 6250-6284. DOI 10.1002/anie.200400655.

[34] Li Y., Hu Y., Zhao Y., Shi G., Deng L., Hou Y. and Qu. L., *Adv. Mater.*, 2011; **23(6)**: 776-780. DOI 10.1002/adma.201003819.

[35] Oliveira M.L.N., Malagoni R.A. and Franco Jr.M.R., *Fluid Phase Equilib.*, 2013; **352**: 110-113. DOI 10.1016/j.fluid.2013.05.014.

[36] Chuhei O. and Ayato N., *J. Phys. Condens. Matter*, 1997; **9(1)**: 1. DOI 10.1088/0953-8984/9/1/004.

[37] Wojnicki M., Fitzner K. and Luty-Blocho M., *J. Colloid Interface Sci.*, 2016; **465**: 190-199. DOI 10.1016/j.jcis.2015.11.066.

[38] Song L., Shi J., Lu J. and Lu C., *Chem. Sci.*, 2015; **6**: 4846-4850. DOI 10.1039/C5SC01416F.

[39] Permatasari F.A., Aimon A.H., Iskandar F., Ogi T. and Okuyama K., *Sci. Rep.-UK*, 2014; **6**: 21042. DOI 10.1038/srep05294.

[40] Li Y., Shu H., Wang S. and Wang J., *J. Phys. Chem. C*, 2015; **119(9)**: 4983-4989. DOI 10.1021/jp506969r.

[41] Thanh T.K.N., Maclean N. and Mahiddine S., *Chem. Rev.*, 2014; **114**: 7610-7630. DOI 10.1021/cr400544s.